

Comparison of Electrical Performance and Stability of Flexible Carbon Nanotube Thin Film Transistors of Different Gate Structures

Chandrashekhar M C¹, K C Narasimhamurthy²

¹Associate Professor, Department of Electronics and Communication Engineering, Sri Siddhartha Institute of Technology, Tumkur, India ²Professor, Department of Telecommunication Engineering, Siddaganga Institute of Technology, Tumkur, India

Abstract: In this work, fabrication of top, bottom and dual-gate carbon nanotube thin film transistors (CNTTFTs) of different dimensions with single-walled carbon nanotubes (SWCNTs) of 99.99% semiconducting purity on a polyimide substrate are reported. Electrical performance comparison of flexible CNTTFTs with different gate structures located at the top, bottom and both at the top and the bottom (dual-gate) of the SWCNTs thin film used as a channel is studied. Top, bottom, and dual-gate CNTTFTs exhibited p-type behavior. Dual-gate CNTTFTs outperformed the bottom-gate and top-gate CNTTFTs of identical dimensions in on-off current ratio, transconductance, drain conductance, subthreshold slope and mobility. Dual-gate and top-gate CNTTFTs exhibited a threshold shift of less than 1.3V and stability in other electrical performance parameters other than threshold voltage without much variation over a time of 60 days exposed to air after fabrication. This work demonstrates that dual-gate CNTTFTs have exhibited better electrical performances and gate control over the channel than the top-gate and bottom-gate CNTTFTs. Dual-gate CNTTFTs are preferred for better electrical performances than top-gate and bottom-gate in flexible applications.

Keywords: Carbon nanotube thin film transistors, dual gate, flexible, on-off current ratio, single-walled carbon nanotubes.

Introduction

Single-walled carbon nanotubes (SWCNTs) in the form of thin-film are used in the channel area of carbon nanotube thin film transistors (CNTTFTs). SWCNTs exhibit high carrier mobility, low operating voltage and are available in solution forms [1-4]. CNTTFTs are fabricated on a wafer scale on silicon (Si) substrates, and electrical performances were studied [5-10]. The researchers are using SWCNTs of higher semiconducting purity, the higher density of deposition and orientation of random or aligned in the fabrication of CNTTFTs to achieve better electrical performances [4,9,11].

Now a days, researchers are fabricating CNTTFTs of different gate structures on flexible substrates like polyimide, polyethylene terephthalate (PET), polyethersulfone (PES), plastic transparency films, polyethylene naphthalate (PEN) to use in flexible applications such as radio frequency identification tags, electronic papers, digital circuits, smart skins, fingerprint scanners, photovoltaics [12-19]. CNTTFTs which exhibit stability on exposure to air after some days following fabrication, lower threshold voltages and lower subthreshold swing are suited in the circuits such as driving circuits of flexible displays and other digital circuits. The electrical characteristics comparison of flexible CNTTFTs with different gate structures is required to decide the better gate structure to be used in flexible applications.

In this work, the top, bottom and dual-gate CNTTFTs on a polyimide substrate are fabricated using photolithography for patterning of electrodes and SWCNTs thin film in the channel area, and their electrical characteristics are compared. The stability of top and dual-gate CNTTFTs was investigated by performing electrical characterization immediately after the fabrication and exposure to air for 60 days following fabrication.

Fabrication Process

Bottom, top and dual-gate CNTTFTs were fabricated on a flexible polyimide substrate. Photolithography and lift-off process was used for patterning of electrodes and SWCNTs thin film between source and drain.

Steps of fabrication of bottom and dual-gate CNTTFTs are illustrated in figure 1(a-i). 6 masks were prepared to use in photolithography for patterning of source, drain and gate electrodes, gate dielectric oxides, and SWCNTs thin film.

Preparation of masks starts with the writing of layouts using Clewin layout editor version 2.8. Then layouts were written on the iron-oxide-coated mask plates by laser writer LW 405 using layouts in GDSII format.

Polyimide tape 5413M with silicone adhesive coated on the bottom side, of thickness 70 μ m, a width of 25.4mm and length of 40 mm was affixed on a silicon wafer. Polyimide substrate fixed on a Si wafer is

shown in figure 1(a). Then before lithography process polyimide substrate was preheated at 90°C for 5 minutes.

The process flow for fabrication of bottom gate CNTTFTs are as follows. The positive photoresist (PPR) S1813 was spin coated on a polyimide substrate. Substrate was preheated at 90°C for 3 minutes, and nitrogen was blown on a mask. Double-sided aligner DSA EVG 620 was used in the process of photolithography. Then the photoresist deposited on polyimide substrate was exposed to ultraviolet (UV) light for 8seconds. Polyimide substrate was kept in MF319 developer solution for 15 seconds to remove softened resists and developed PPR is shown in figure 1(b).

Titanium/gold (Ti/Au) bottom gate of metal of thickness 7/50nm was deposited by 4 target E-beam evaporator (4-TEBE) and patterned using photolithography is shown in figure 1(c). Hafnium dioxide (HfO₂) dielectric layer of 10nm thickness was deposited by radio frequency (RF) sputtering, patterned using photolithography and resulting cross-sectional view is shown in figure 1(d).

Next process was SWCNTs deposition on the HfO₂ to form a thin film of SWCNTs. SWCNTs solution obtained from Nano Integris Inc., USA was used for thin film deposition. The solution contained 99.99% semiconducting purity SWCNTs. The solution obtained was in the form of an aqueous surfactant solution with a concentration of 1.0 mg SWCNTs in 25 ml solution. To increase the density of nanotubes on silicon dioxide(SiO₂) surface, the SiO₂ surface was amino isopropyl triethoxysilane(APTES) [12,-14] functionalized.

The following procedure for APTES functionalization was followed. The polyimide substrate was immersed in sulphochromic acid for 2 minutes and then rinsed in deionized water thoroughly to create OH bonds and dried using nitrogen (N₂) gas. The polyimide substrate was heated for 1 hour at 120°C and 10⁻²mbar pressure. A solution containing 60micro liter of 3-aminoisopropyltriethoxysilane and 20 ml of isopropyl alcohol [IPA] was prepared. The polyimide substrate was immersed in this prepared solution for 15 minutes in argon ambient. The ambient was created in a chamber by filling argon as an inert gas to prevent the polymerization of APTES. Next, the polyimide substrate was rinsed in IPA and dried using Argon gas to complete the process of amino isopropyl triethoxysilane functionalization of the HfO₂ surface. Then the polyimide substrate was immersed in SWCNT solution for 30minutes. To remove sodium dodecyl sulphate (SDS) residual on CNTs, polyimide substrate was rinsed in IPA, followed by a rinse of de-ionized (DI) water and dried with nitrogen gas.

Unwanted SWCNTs outside channel region were removed by oxygen (O₂) plasma etching. The photolithographic steps were used to protect SWCNTs in the channel region. The schematic view of SWCNTs thin film after patterning is shown in figure 1(e).

To realize source and drain contacts of CNTTFTs the palladium/gold (Pd/Au) of 8/20nm thickness was deposited by 4TEBE and patterned using photolithography. The resulting cross-sectional view is shown in figure 1(f). To define more substantial area source, drain, and gate electrode contact pads on polyimide substrate Ti/Au of thickness 7/50nm was deposited by RF sputtering, and a lift-off process removed Ti/Au from unwanted regions. Resultant cross-sectional view of fabricated bottom-gate CNTTFT is shown in figure 1(g).

Dual-gate CNTTFTs were fabricated using two additional steps after the fabrication of bottom-gate CNTTFTs. For top-gate dielectric, SiO₂ of thickness 10nm was patterned using photolithography is shown in figure 1(h). The Ti/Au top-gate of thickness 7/50 nm was patterned using photolithography is shown in figure 1 (i).

The process flow for fabrication of bottom-gate CNTTFTs with SiO₂ as a gate dielectric is same as CNTTFTs fabrication using HfO₂ as a gate dielectric, except HfO₂ deposition and patterning, the SiO₂ was used as dielectric and patterned as shown in step 1(h). CNTTFTs fabricated are of channel length (L) varying from 3 to 100 μm and channel width (W) varying from 3 to 50 μm.

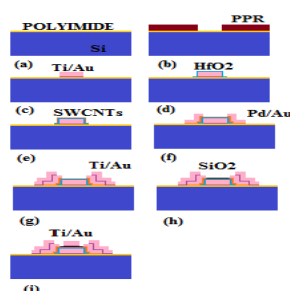


Figure 1. Process steps for fabrication of bottom-gate and dual-gate CNTTFTs. (a) Polyimide substrate pasted on Si wafer. (b) Developed PPR. (c) Patterned Ti/Au gate. (d) Patterned gate dielectric HfO_2 . (e) Patterned SWCNTs put on APTES functionalized HfO_2 . (f) Patterned Pd/Au for source and a drain electrode (g) Patterned Ti/Au to form substantially significant space source, drain and gate contact pads. (h) Patterned top gate dielectric SiO_2 of dual-gate CNTTFT. (i) Patterned top-gate metal Ti/Au of dual-gate CNTTFT.

Method of fabrication of top-gate CNTTFTs is shown in figure 2(a)-2(g). Polyimide tape 5413M with silicone adhesive coated on bottom side, of thickness $70\mu\text{m}$, a width of 25.4mm and length of 40mm was pasted on Si wafer of 2 inches. Polyimide substrate pasted on Si wafer was preheated at 90°C for 5 minutes before lithography process. HfO_2 of thickness 10nm deposited all over the polyimide substrate using RF sputtering as shown in figure 2.3(b). Subsequently, SWCNTs were placed to constitute a thin film of SWCNTs over the HfO_2 surface. The HfO_2 surface was APTES [16-18] functionalized prior to the SWCNTs deposition to increase the density of SWCNTs deposited.

The same procedure for APTES functionalization of the dielectric surface as that was followed in above mentioned bottom-gate fabrication process.

Unwanted SWCNTs outside channel region were depleted by O_2 plasma etching employing photolithographic methods to protect SWCNTs in a channel region as given in figure 2.3(c). 4-TEBE deposited source and drain electrodes were of metal Pd/Au of thickness $8/20\text{nm}$. Placed metal Pd/Au was patterned by standard photolithography, and lift-off process is viewed in figure 2.3(d). The HfO_2 dielectric layer of 10nm thickness was placed by RF sputtering. Placed HfO_2 was patterned employing photolithography, and the resulting cross-sectional view is shown in figure 2.3(e). 4-TEBE deposited Ti/Au top-gate metal of thickness $7/50\text{nm}$. Ti/Au metal was patterned using photolithography is appeared in figure 2.3(f). More substantial area source, drain, and gate electrode contact pad regions of metal Ti/Au of thickness $7/50\text{nm}$ was deposited by RF sputtering on a polyimide substrate. Deposited metal Ti/Au was eliminated from undesired areas by photolithography and lift-off process. Patterned more substantial area source, drain, and gate electrode contact pads of metal Ti/Au are shown in figure 2.3(g).

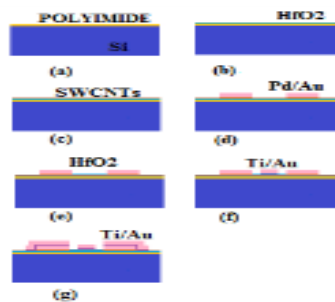


Figure 2. Process steps for fabrication of top-gate CNTTFTs. (a) Polyimide substrate pasted on the Si wafer. (b) HfO_2 deposited on a polyimide substrate. (c) SWCNTs placed on APTES functionalized HfO_2 . (d) Patterned Pd/Au for source and drain electrode. (e) Patterned top-gate dielectric HfO_2 . (f) Patterned Ti/Au gate. (g) Patterned Ti/Au for extensive area source, drain and gate contact pads.

After the fabrication of CNTTFTs on a polyimide substrate the substrate was peeled-off from the Si wafer. After it was peeled off from Si wafer the photograph of polyimide substrate that was held with hands is shown in figure 3.



Figure 3. Polyimide substrate peeled-off from Si substrate after CNTTFTs fabrication.

Results and Discussion

In this section discussion on images of SWCNTs deposited taken by field emission scanning electron microscope (FESEM), Raman spectroscopy data of SWCNTs thin-film deposited on gate oxide and the study of comparison of electrical characteristics, electrical parameters such as maximum on current (I_{ON}) on-off current ratio ($I_{\text{ON}}/I_{\text{OFF}}$), transconductance (g_m), drain conductance (g_{ds}), carrier mobility (μ_{carr}) and threshold voltage (V_{th}) of flexible top, bottom and dual-gate CNTTFTs. Also, the investigation on the stability of

flexible top and dual-gate CNTTFTs, when exposed to air for a time duration of 60 days after the fabrication was done.

FESEM image was taken to find the density of SWCNTs placed on a polyimide substrate as shown in figure 4. The density of SWCNTs deposited is around 70 nanotubes/ μm^2 . Raman spectroscopy data was used to evaluate the semiconducting purity of SWCNTs and to find whether the presence of metallic nanotubes is lower or higher [20]. Radial breathing modes (RBM) first-order and second-order Raman frequencies (150–350 cm^{-1}) provide the data of diameter, chirality, and phonon structure. Graphene plane graphite band (1565–1595 cm^{-1}) gives data of carbon-carbon stretching. The RBM and G-modes remain affected by diameter. Raman spectra of SWCNTs deposited on APTES functionalized SiO_2 dielectric surface have appeared in figure 5. The tops of radial breathing modes, the disordered band (D band), graphite band (G band) and G' band are shown in figure 5. RBM regions of SWCNTs provide qualitative proof of a relative population of semiconducting to metallic nanotubes put over the surface. Raman peaks at about 160–200 cm^{-1} and 200–280 cm^{-1} are due to semiconducting and metallic SWCNTs respectively [21]. Raman spectroscopy RBM data shows peaks at a Raman shift less than 200 cm^{-1} which demonstrates the highest semiconducting purity of SWCNTs and absence of metallic nanotubes in SWCNTs. Microscopic pictures of the flexible top-gate CNTTFTs fabricated on a polyimide substrate are shown in figure 6. Microscopic image of a fabricated flexible top-gate CNTTFT of $L=5\mu\text{m}$, $W=40\mu\text{m}$ is shown in figure 7.

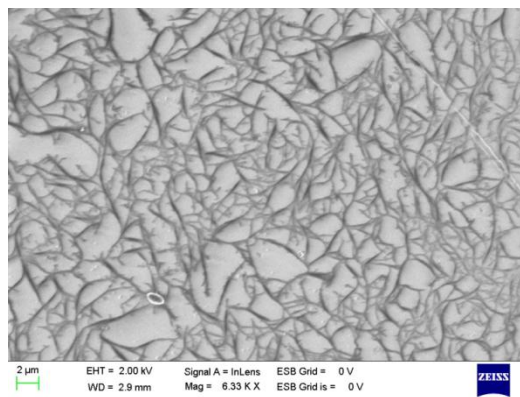


Figure 4. FESEM image of a thin-film of SWCNTs deposited between electrodes of CNTTFTs on a polyimide substrate to form a channel.

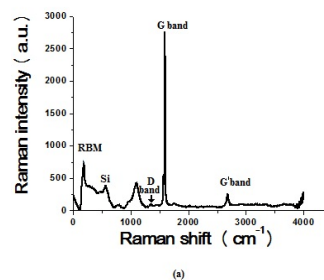


Figure 5. Raman spectroscopy data of placed SWCNTs thin film.



Figure 6. The microscopic picture of a flexible top-gate CNTTFTs.

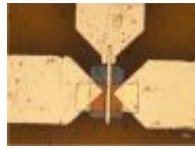


Figure 7. Microscope picture of a fabricated flexible top-gate CNTTFT of $L=5\mu\text{m}$, $W=40\mu\text{m}$.

Output and transfer characteristics of dual, bottom and top-gate flexible CNTTFT of $L=8\mu\text{m}$, $W=5\mu\text{m}$ are shown in figure 8. Gate dielectrics employed in dual-gate flexible CNTTFTs are HfO_2 and SiO_2 of thickness 40nm each, whereas top-gate and bottom-gate flexible CNTTFTs employ HfO_2 of thickness 40nm. Output characteristics taken by the varying drain to source voltage (V_{DS}) at constant gate voltages (V_{GS}) are shown in figures 8(a), 8(b), 8(c) correspondingly for dual, bottom and top-gate CNTTFTs. Dual-gate CNTTFTs showed p-type characteristics as shown in figure 8(a). Dual-gate CNTTFT has shown maximum on current of $63.9\mu\text{A}$ at constant $V_{\text{GS}} = -50\text{V}$. The saturation voltage is reached at a voltage $V_{\text{DS}} = -42\text{V}$ for a constant voltage of $V_{\text{GS}} = -50\text{V}$. Estimated drain conductance for a device at $V_{\text{GS}} = -20\text{V}$ is $0.96\mu\text{S}$. Top and bottom-gate CNTTFTs also presented p-type features as viewed from figures 8(c) and 8(e).

Bottom-gate CNTTFT has shown a peak on current of $30.7\mu\text{A}$ at constant $V_{\text{GS}} = -50\text{V}$. The saturation voltage is attained at a voltage $V_{\text{DS}} = -40\text{V}$ for a constant voltage of $V_{\text{GS}} = -50\text{V}$. Estimated drain conductance for a CNTTFT at $V_{\text{GS}} = -20\text{V}$ is $1.02\mu\text{S}$ as viewed from figure 8(c).

The top-gate CNTTFT has displayed a peak on current of $17.2\mu\text{A}$ at constant $V_{\text{GS}} = -50\text{V}$. The saturation voltage is reached at a voltage $V_{\text{DS}} = -39\text{V}$ for a constant voltage of $V_{\text{GS}} = -50\text{V}$. Estimated drain conductance for a CNTTFT at $V_{\text{GS}} = -20\text{V}$ is $1.1\mu\text{S}$ as seen from figure 8(e).

Study of output characteristics of flexible CNTTFTs of various gate arrangements confirmed that dual-gate CNTTFTs have a higher peak on current and less value of drain conductance than bottom-gate and top-gate CNTTFTs because of the better control of the channel than other two. Between flexible bottom and top-gate CNTTFTs, flexible bottom-gate CNTTFTs have displayed a higher amount of peak on current and weaker drain conductance.

The carrier mobility is calculated applying equation (1)

$$\mu_{\text{carr}} = L g_m / V_{\text{DS}} C_{\text{ox}} W \quad (1)$$

where C_{ox} is the gate capacitance per unit area determined considering into account electrostatic coupling among nanotubes and utilizing formula reported in [22-24].

The transfer characteristics for various voltages V_{GS} of dual, bottom and top-gate CNTTFTs of $L=8\mu\text{m}$, $W=5\mu\text{m}$ correspondingly are given in figures 8(b), 8(e), 8(b), respectively. On current from the transfer characteristics of dual-gate CNTTFT as seen from figure 8(b) is $27.2\mu\text{A}$ at constant $V_{\text{DS}} = -20\text{V}$. At constant V_{DS} of -20V obtained values of on-off current ratio, transconductance, subthreshold swing, threshold voltage and mobility of dual-gate CNTTFT correspondingly are 9.65×10^4 , $0.6\mu\text{S}$, 172.08mV/decade , -1V and $0.2136\text{cm}^2/\text{Vs}$.

On current estimated from transfer characteristics of bottom-gate CNTTFT is shown in figure 8(d) is $13.1\mu\text{A}$ at constant $V_{\text{DS}} = -20\text{V}$. At constant V_{DS} of -20V deduced values of on-off current ratio, transconductance, subthreshold swing, threshold voltage and mobility of bottom-gate CNTTFT correspondingly are 1.6375×10^4 , $0.20\mu\text{S}$, 321.54mV/decade , -2V and $0.08667\text{cm}^2/\text{Vs}$.

On current from transfer characteristics of top-gate CNTTFT is viewed in figure 8(f) is $5.08\mu\text{A}$ at constant $V_{\text{DS}} = -25\text{V}$.

At constant V_{DS} of -25V the deduced values of on-off current ratio, transconductance, subthreshold swing, threshold voltage and mobility of top-gate CNTTFT correspondingly are 1.668×10^3 , $0.20\mu\text{S}$, 321.54mV/decade , -2.5V and $0.1414\text{cm}^2/\text{Vs}$.

Dual-gate CNTTFT has displayed better steep subthreshold swing, higher on-off current ratio, better transconductance contrasted to the top and bottom-gate CNTTFTs. Dual-gate CNTTFTs surpassed single-gate CNTTFTs in electrical performance because of the higher authority of channel area between the source and drain electrodes since dual-gate devices have two gates.

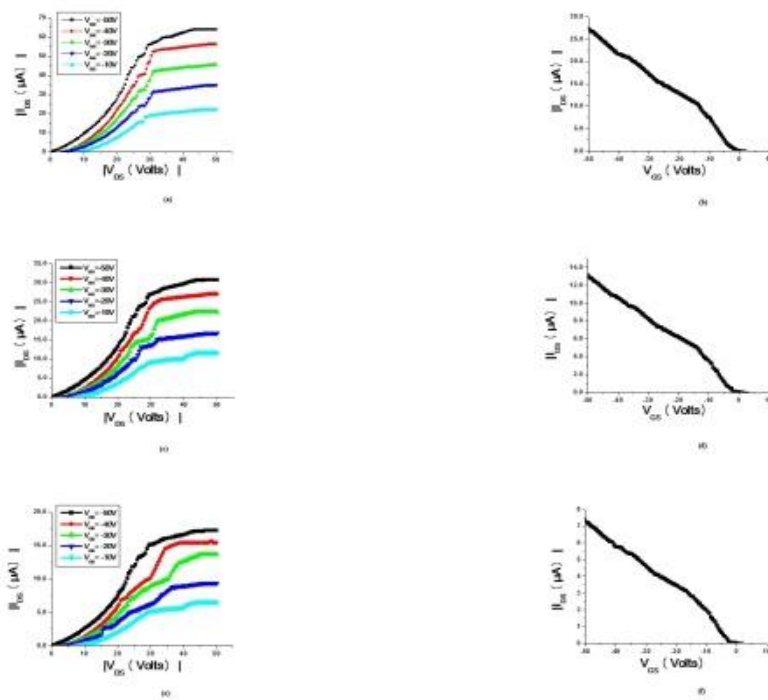


Figure8. Output and transfer characteristics of flexible CNTTFT of channel length equal to $8\mu\text{m}$, channel width equal to $5\mu\text{m}$ for various gate arrangements. Output characteristics of (a) Dual-gate. (c) Bottom-gate. (e) Top-gate. Transfer characteristics of (b) Dual-gate. (d) Bottom-gate. (f) Top-gate.

Stability as a function of time after the fabrication of CNTTFTs is studied for dual-gate flexible CNTTFT of $L=15\mu\text{m}$, $W=5\mu\text{m}$. Transfer characteristics of dual-gate flexible CNTTFT plotted immediately after fabrication and exposure to air for 60 days later fabrication is presented in figure 9. Other than threshold voltage electrical performance of flexible CNTTFT is not degraded significantly. The shift in threshold voltage shift is 1.3V . Degradation of electrical performance parameters is not displayed because of encapsulation of SWCNTs thin-film by two gates to air.

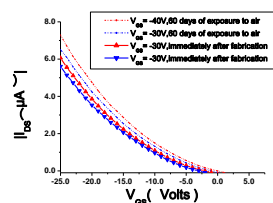


Figure 9. Transfer characteristics of flexible dual-gate CNTTFT of $L=15\mu\text{m}$, $W=5\mu\text{m}$ measured immediately after the fabrication and exposure to air for 60 days after the fabrication.

Stability as a function of time after the fabrication of CNTTFTs is studied for top-gate flexible CNTTFT of $L=5\mu\text{m}$, $W=5\mu\text{m}$. Transfer characteristics of top-gate flexible CNTTFT plotted immediately after fabrication and exposure to air for 60 days later fabrication is presented in figure 10. Other than threshold voltage electrical performance of flexible CNTTFT is not degraded significantly. The shift in threshold voltage shift is 1V . Degradation of electrical performance parameters is not displayed because of encapsulation of SWCNTs thin-film by a gate to air.

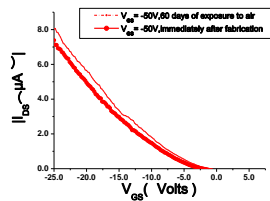


Figure 10. Transfer characteristics of flexible top-gate CNTTFT of $L=5\mu\text{m}$, $W=5\mu\text{m}$ measured immediately after the fabrication and exposure to air for 60 days after the fabrication.

When compared to the dual-gate flexible CNTTFTs shift in threshold voltage of top-gate flexible CNTTFTs is lesser because the area of SWCNTs thin-film exposed in the gaps separating gate structure, and source and drain electrodes is lesser since it is a single gate.

Stability as a function of time after the fabrication of CNTTFTs exhibits no significant degradation in electrical performance is displayed by both dual-gate and top-gate flexible CNTTFTs but exhibited a threshold shift of lesser than 1.3V.

Conclusion

In the present work, top, bottom and dual-gate carbon nanotube thin film transistors of various dimensions with single-walled carbon nanotubes of 99.99% semiconducting purity on a polyimide substrate were fabricated. Electrical performance of flexible CNTTFTs with various gate arrangements was compared. Top, bottom, and dual-gate CNTTFTs showed p-type performance. Dual-gate CNTTFTs bettered the bottom and top-gate CNTTFTs of identical dimensions in on-off current ratio, transconductance, drain conductance, subthreshold slope and mobility. Dual and top-gate CNTTFTs shown threshold shift of less than 1.3V and stable in rest of electrical performance parameters other than threshold voltage without much variation when exposed to air for 60 days later fabrication. Present work investigated that dual-gate CNTTFTs exhibited better electrical performances and gate control over channel than top and bottom-gate CNTTFTs. The dual-gate CNTTFTs are preferred for better electrical performances than top and bottom-gate inflexible uses.

Acknowledgment

This work was carried out at the Centre of Excellence in Nanoelectronics (CEN) at Indian Institute of Technology Bombay (IITB) with financial support from Indian Nanoelectronics Users Program (INUP) initiated by Department of Information Technology (DIT), Ministry of Communications and Information Technology (MCIT), Government of India. The authors thank Professors and Staff members of CEN, IITB, for their valuable suggestions and support.

References

- [1]. Daniel Pham, Harish Subbaraman, Maggie Yihong Chen, Xiaochuan Xu, and Ray T. Chen "Bending Tests of Carbon Nanotube Thin-film Transistors on Flexible Substrate" Article in Proc SPIE · Vol.7761, 8 pages, August 2010, DOI: 10.1117/12.864066.
- [2]. Sukjae Jang, Houk Jang, Youngbin Lee, Daewoo Suh, Seunghyun Baik, Byung Hee Hong, and Jong-Hyun Ahn, "Flexible, transparent single-walled carbon nanotube transistors with graphene electrodes". Nanotechnology, Vol.21, No.42, pp.425201-425205, October 2010.
- [3]. Xuan Cao, Haitian Chen, Xiaofei Gu, Bilu Liu, Wenli Wang, Yu Cao, Fanqi Wu, and Chongwu Zhou, "Screen Printing as a Scalable and Low-Cost Approach for Rigid and Flexible Thin-Film Transistors Using Separated Carbon Nanotubes" ACS Nano, Vol.8, NO. 12, pp. 12769-12776, December 2014.
- [4]. Fumiaki N. Ishikawa, Hsiao-kang Chang, Kounghmin Ryu, Po-chiang Chen, Alexander Badmaev, Lewis Gomez, De Arco, Guozhen Shen, and Chongwu Zhou, "Transparent Electronics Based on Transfer Printed Aligned Carbon Nanotubes on Rigid and Flexible Substrates". ACS Nano, Vol. 3, NO. 1, pp.73-79, 2009
- [5]. M. C. LeMieux, S. Sok, M. E. Roberts, J. P. Opatkiewicz, D. Liu, S. N. Barman, N. Patil, S. Mitra, and Z. Bao, "Solution Assembly of Organized Carbon Nanotube Networks for Thin-film Transistors," ACS Nano, Vol. 3, No. 12, pp. 4089-4097, December 2008.
- [6]. H. Ko and V. V. Tsukruk, "Liquid-crystalline processing of highly oriented carbon nanotube arrays for thin-film transistors," Nano Lett., Vol. 6, No. 7, pp. 1443-1448, July 2006.
- [7]. K.C. Narasimhamurthy, Roy Paily, "Performance comparison of interdigitated thin-film-field effect transistors using different purity semiconducting carbon nanotubes", Advanced Materials Research, Vol.181-182, pp343-348, January 2011.

- [8]. M. C. LeMieux, M. Roberts, S. Barman, Y. W. Jin, J. M. Kim, and Z. Bao, "Self-sorted, Aligned Nanotube Networks for Thin-film Transistors," *Science*, Vol. 321, No. 5885, pp. 101–104, August 2008.
- [9]. K.C.Narasimhamurthy,Roy Paily, "Wafer Scale Thin-film Transistors Using Different Semiconducting Purity Nanotubes, Dielectric Materials and Gate Control", *Solid State Electronics*,Vol.79,pp.37–44, January 2013.
- [10].C. Wang, J. Zhang, K. Ryu, A. Badmaev, L. G. D. Arco, and C. Zhou,"Wafer-scale fabrication of separated carbon nanotube thin-film transistors for display applications," *Nano Lett.*, Vol. 9, No. 12, pp. 4285–4291, November 2009.
- [11].M. Engel, J. P. Small, M. Steiner, M. Freitag, A. A. Green, M. C. Hersam,and P. Avouris, "Thin Film Nanotube Transistors Based on Self-assembled,Aligned, Semiconducting Carbon Nanotube Arrays," *ACS Nano*, Vol. 2, No. 12, pp. 2445–2452, December2008.
- [12].Chandra, B., Park, H., Maarouf, A., Martyna, G. J. & Tulevski, G. S. "Carbon nanotube thin film transistors on flexible substrates", *Appl. Phys. Lett.* Vol.99, No.7,72110-72113, August 2011.
- [13].Pingqi Gao,Qing Zhang, "Encapsulate-and-Peel: Fabricating Carbon Nanotube CMOS Integrated Circuits in a Flexible Ultra- Thin Plastic Film,"*Nanotechnology*,Vol. 25, No.6,pp.065301-065307,January2014.
- [14].Jianshi Tang , Qing Cao, George Tulevski, Keith A. Jenkins, Luca Nela, Damon B. Farmer and Shu-Jen, "Flexible CMOS Integrated Circuits Based on Carbon Nanotubes with Sub-10 ns Stage Delays," *Nature Electronics Articles*, Vol 1, pp.191–196,March 2018.
- [15].Rogers J A et al,"Paper-like Electronic Displays:Large-area Rubber–Stamped Plastic Sheets of Electronics and Microencapsulated Electrophoretic Inks," *Proc. Natl. Acad. sci.*,Vol.98,No.9, pp.4835-4840,April 2001.
- [16].Dodabalapur A,"Organic and Polymer Transistors for Electronics" *Materials Today*, Vol. 9,No.4,pp.24-30,April 2006.
- [17].Someya T, Kato Y,Sekitani T,Iba S,Noguchi Y,Murase Y, Kawaguchi H and Sakurai T,"Conformable, Flexible ,Large Area Networks of Pressure and Thermal Sensors with Organic Transistor Active Matrixes", *Proc.Natl. Acad. Sci.*, Vol.102, pp.12321-12325,August2005.
- [18].Chandrashekhar M C and K C Narasimhamurthy, "Fabrication, Electrical Characterization and Mechanical Flexibility Test of Back Gated Carbon Nanotube Thin Film Transistors on Polyimide Substrate," *Materials Research Express*, Vol.5, No.12, pp.126304-126310, September 2018.
- [19].Someya T,Sekitani T,Iba S,Kato Y,Kawaguchi H and Sakurai T,"A Large–area, Flexible Pressure Sensor Matrix with Organic Field –Effect Transistors for Artificial Skin Applications," *Proc.Natl.Acad.Sci.USA*,Vol.101,No.27, 9966-1019970,July2004.
- [20].M. Engel, J. P., Small, M. Steiner, M. Freitag, A. A. Green, M. C. Hersam, and P. Avouris, "Thin Film Nanotube Transistors Based on Self-assembled, Aligned, Semiconducting Carbon Nanotube Arrays," *ACS Nano*,Vol.2,No.12, pp.2445-2452,December 2008.
- [21].H Kataura, Kumazawa, Y.Maniwa, I Umezu,S Suzuki,Y Ohtsuka, and Y achiba, "Optical properties of single-wall carbon nanotubes", *Synth. Met.* Vol.103, No.1-3, pp.2555-2558, June1999.
- [22].Kang,S.J.,Kocabas,C.,Ozel,T.,Shim,M.,Pimparkar,N.,Alam,M.A.,Rotkin,S.V.,Rogers,J.A,"High-Performance Electronics Using Dense, Perfectly Aligned Arrays of Single-walled Carbon Nanotubes," *Nature Nanotechnology*, Vol.2, pp.230-236,March 2007.
- [23].Cao,Q.,Xia,M., Kocabas, C.,Rogers,J.A., and Rotkin S.V, "Gate capacitance coupling of single-walled carbon nanotube thin-film transistors," *Appl. Phys .Lett.* ,Vol.90, pp.023516-1- 023516-3, January 2007.
- [24].Chuan Wang, Jialu Zhang, and Chongwu Zhou, "Macro electronic integrated circuits using high- performance separated carbon nanotube thin film transistors," *ACS Nano*,Vol.4, No.12, pp.7123-7132,November.2010.